Geological structure, recharge processes and underground drainage of a glacierised karst aquifer system, Tsanfleuron-Sanetsch, Swiss Alps

Vivian Gremaud · Nico Goldscheider · Ludovic Savoy · Gérald Favre · Henri Masson

Abstract The relationships between stratigraphic and tectonic setting, recharge processes and underground drainage of the glacierised karst aquifer system 'Tsanfleuron-Sanetsch' in the Swiss Alps have been studied by means of various methods, particularly tracer tests (19 injections). The area belongs to the Helvetic nappes and consists of Jurassic to Palaeogene sedimentary rocks. Strata are folded and form a regional anticlinorium. Cretaceous Urgonian limestone constitutes the main karst aquifer, overlain by a retreating glacier in its upper part. Polished limestone surfaces are exposed between the glacier front and the end moraine of 1855/1860 (Little Ice Age); typical alpine karrenfields can be observed further below. Results show that (1) large parts of the area are drained by the Glarey spring, which is used as a drinking water source, while marginal parts belong to the catchments of other springs; (2) groundwater flow towards the Glarey spring occurs in the main aquifer, parallel to stratification, while flow towards another spring crosses the entire stratigraphic sequence, consisting of about 800m of marl and limestone, along deep faults that were probably enlarged by mass movements; (3) the variability of glacial meltwater production influences the shape of the tracer breakthrough curves and, consequently, flow and transport in the aquifer.

Keywords Karst · Retreating glacier · Multi-tracer test · Climate change · Switzerland

Received: 13 November 2008 / Accepted: 12 May 2009
Published online: 16 June 2009

V. Gremaud · N. Goldscheider (✉)
Centre of Hydrogeology,
University of Neuchâtel,
Rue Emile-Argand 11, CP 158, 2009, Neuchâtel, Switzerland
e-mail: nico.goldscheider@unine.ch
Tel.: +41-32-7182645
Fax: +41-32-7182603

L. Savoy
Hydro-Geol Sàrl,
POB 2430, 2001, Neuchâtel, Switzerland

G. Favre
Geologos SA,
16 route de Crassier, 1277, Borex, Switzerland

H. Masson
Institut de Géologie et Paléontologie,
Université de Lausanne,
1015, Lausanne, Switzerland

Introduction

The Alps are often considered as the 'water towers of Europe'. Just as in most other high mountain areas, annual precipitation is substantially higher than in the surrounding lowlands; the snow that falls in the cold season is retained in snowfields and glaciers, from which it is slowly released during warmer periods to provide large volumes of freshwater to springs, streams, rivers and aquifers (e.g. Viviroli and Weingartner 2004).

Nowhere in Central Europe is climate change so obvious as in the Alps, where rapidly retreating glaciers are the most visible expression of a changing climate (Greene et al. 1999; Paul et al. 2004). Relatively little research has been done on the current and future impacts of climate change on the alpine water resources. Available studies suggest that, during the winter, warmer temperatures and more precipitation in the form of rain instead of snow are likely to result in more available freshwater, while less rain in summer, along with the shrinking or disappearance of glaciers, may result in local, temporary water shortage, particularly in late summer (Kleinn et al. 2005; Schaefli et al. 2007; Seidel et al. 1998).

There are few places in the Alps where the interrelations between climate change, retreating glaciers, groundwater resources and freshwater supply are so immediate as in the Tsanfleuron-Sanetsch region in western Switzerland, where a rapidly retreating glacier (Tsanfleuron glacier) directly overlies and recharges the upper part of a large regional karst aquifer (Fig. 1), which is drained at its lowest point by a spring (Glarey spring) used for the drinking water supply of a community (Conthey), as well as for irrigation purpose. Therefore, a research project was set up to study this alpine glacier and karst aquifer system.

DOI 10.1007/s10040-009-0485-4

Fig. 1 Impression of the upper part of the Tsanfleuron-Sanetsch area, where the rapidly retreating Tsanfleuron glacier directly overlies and recharges the Cretaceous limestone karst aquifer (photo: N. Goldscheider)

A few available studies focus on glacier-groundwater interactions, mostly numerical modelling of large-scale flow beneath recent or Pleistocene ice shields (Flowers et al. 2003; Boulton et al. 1993), as well as long-term simulations evaluating the role of infiltrating meltwaters for the cooling of alpine massifs (Maréchal et al. 1999). Very few researchers have studied the relations between alpine glaciers and connected karst aquifers (Smart 1996).

The Tsanfleuron-Sanetsch area belongs to a long chain of karst aquifer systems developed in the Helvetic zone of the Alps, mostly in a Cretaceous limestone formation known as *Schrattenkalk* (German) or *Urgonian* (French). Well-studied examples include the Muotathal area, which encompasses the Hölloch, the longest cave in the Alps (Jeannin 2001); the Siebenhengste-Hohgant area with the second longest cave in the Alps (Häuselmann et al. 2003); and the Hochifen-Gottesacker area, a prime example of a karst system where fold structures were demonstrated to have a major influence upon the underground drainage pattern (Goldscheider 2005). The Tsanfleuron-Sanetsch area, on the other hand, has received little attention from hydrogeologists, while glaciologists and sedimentologists have studied the glacier and its forefield (Fairchild et al. 1999; Hubbard 2002; Hubbard et al. 2003; Hubbard et al. 2000).

The relationships between geological structure and underground drainage pattern of this test site were studied during a first project phase from 2004 to 2008. The fieldwork included geological mapping, hydrological observations, and 19 tracer injections. The primary goals were to identify the main karst springs, to delineate their catchment areas and to determine linear groundwater flow velocities. The study has also revealed new insights into the influence of nappe boundaries, folds structures and deep faults on groundwater flow, as well as insights into the unique recharge processes in glacierised karst aquifer systems. Furthermore, several observations indicate deep infiltration into large, gravity-driven flow systems, in accordance with the conceptual models proposed by Toth (1963, 1999).

On this basis, a second project phase will focus on the influence of the glacier and snowmelt on the diurnal and seasonal variability of groundwater flow and glacier-born turbidity. The third project phase will aim to make prognoses concerning the possible impact of climate-change induced glacier retreat on aquifer dynamics and freshwater availability.

Geologic setting and karst development

Geologic framework and nappe tectonics

The Tsanfleuron-Sanetsch area belongs to the Helvetic domain of the Alps and is formed by a pile of several nappes made of Mesozoic and Paleogene rocks, among which limestones play an important role. The region is a classical example of nappe tectonics (Lugeon 1914). The present geologic knowledge and terminology were established by Lugeon (1940), Badoux et al. (1959, 1990), Escher et al. (1993) and Steck et al. (1999, 2001).

Large parts of the study area are formed by the Diablerets nappe, while the adjacent areas to the N, E and SE belong to the overlying Mont-Gond nappe (Figs. 2 and 3). In the study area, the Diablerets nappe is generally little deformed, while the Mont-Gond nappe has a thin and strongly deformed overturned limb that is connected to the Diablerets nappe by an isoclinal syncline. Its hinge is clearly discernible south of Tsanfleuron near the Glarey spring (Fig. 3).

 DOI 10.1007/s10040-009-0485-4

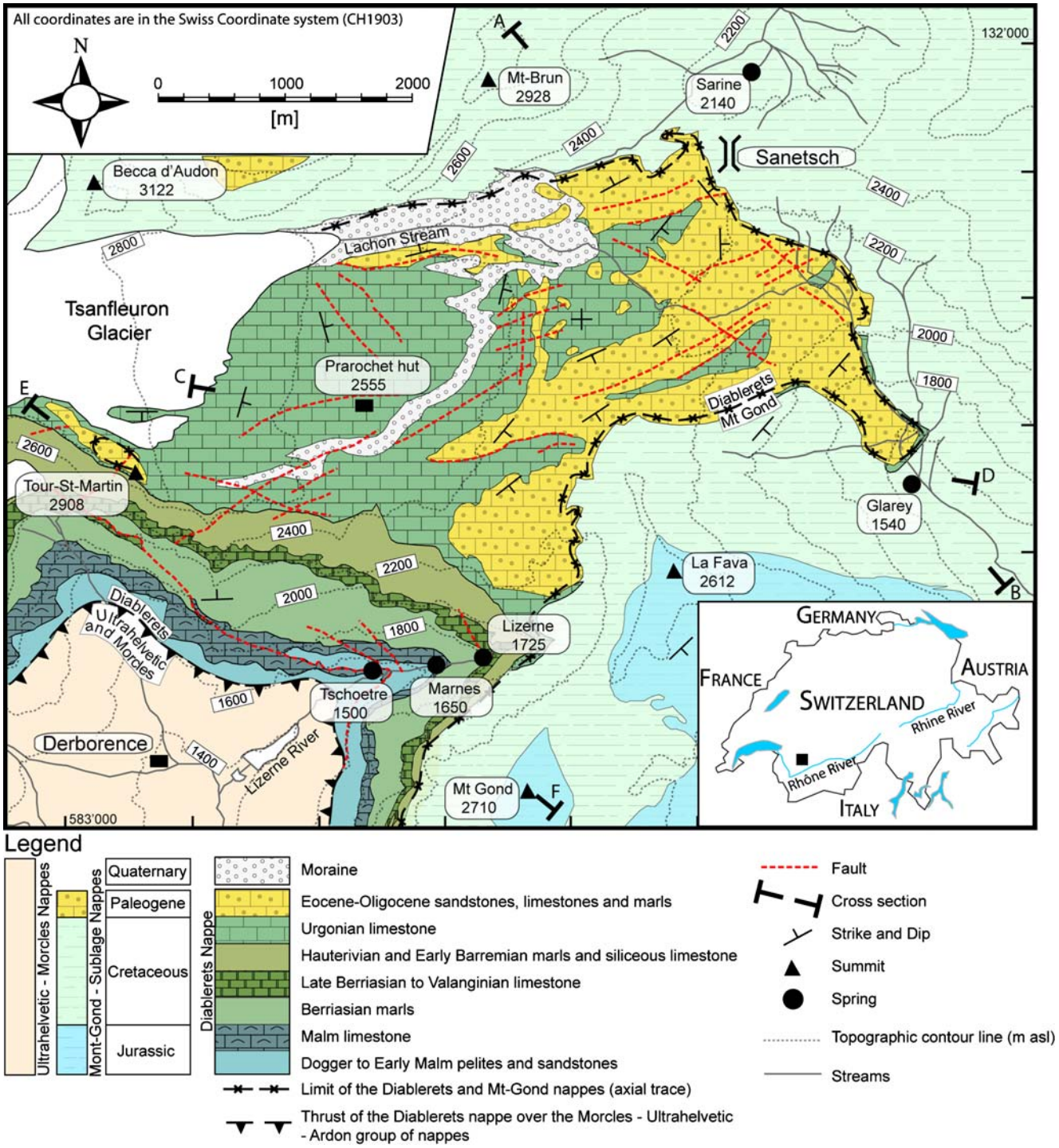

Fig. 2 Geologic map of the Tsanfleuron-Sanetsch area (with Swiss coordinates). Large parts of the study area belong to the Diablerets nappe and mainly consist of Cretaceous Urgonian limestone. The stratigraphy of the over- and underlying nappes is strongly simplified. Relevant springs and streams are also shown; elevations are in meters above sea level

The basal thrust of the Diablerets nappe follows a Middle Jurassic (Aalenian) clay formation known for its ductility and low permeability (e.g. Crespo-Blanc et al. 1995). The tectonic complex below includes parts of the Morcles nappe and several other units. The top of the Morcles nappe is formed by thick and clayey Oligocene flysch. For these reasons, it can be assumed that the Diablerets and Morcles nappes form two separated hydrogeologic systems.

The entire pile of nappes is gently folded and forms a huge anticlinorium in the Tsanfleuron-Sanetsch area (Steck et al. 2001). The axial plunge of this structure is between 5 and 10° to the ENE. The dips of the strata rarely exceed 10° to the NW and 25° to the SE.

 DOI 10.1007/s10040-009-0485-4

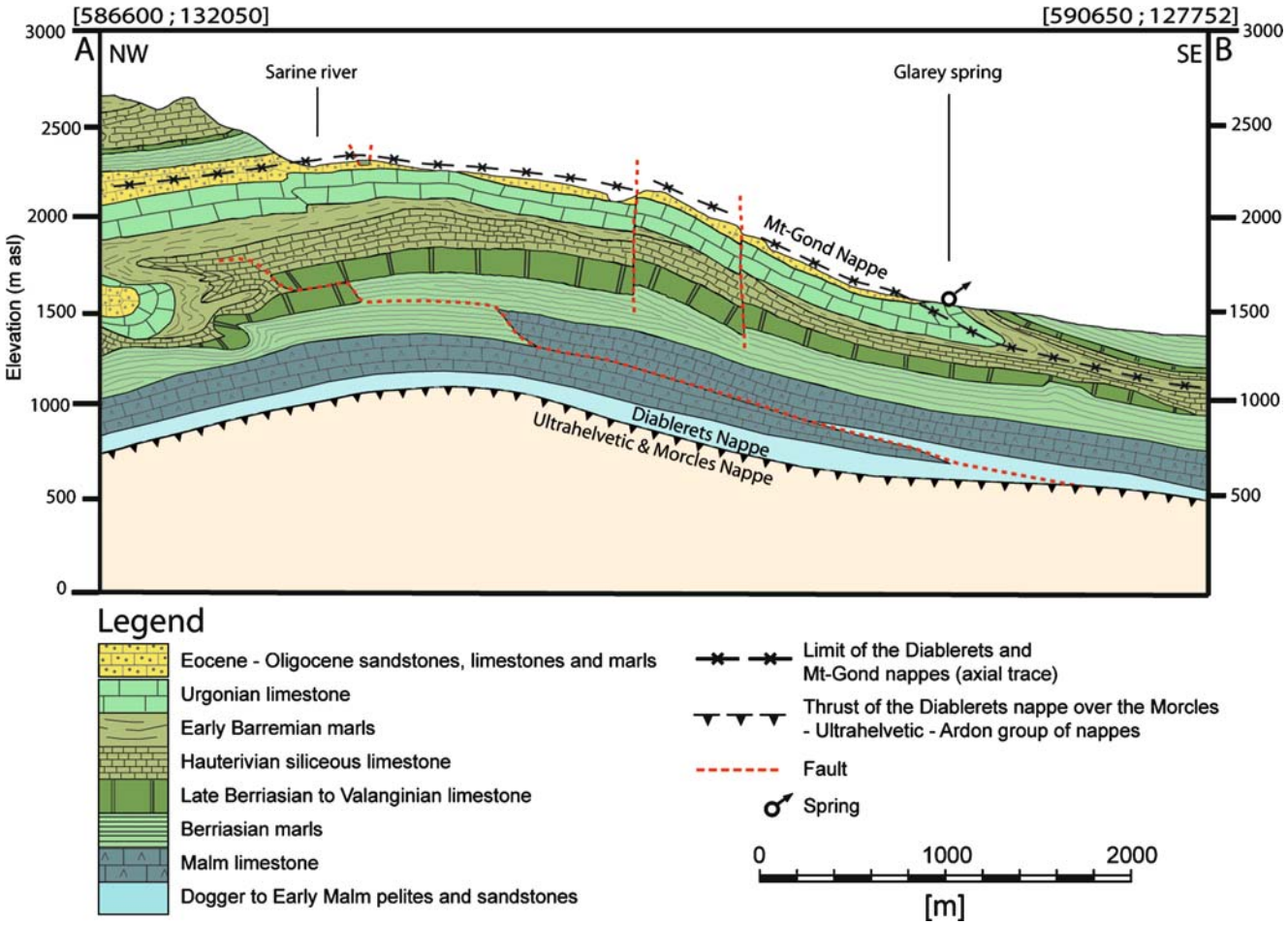

Fig. 3 Cross-sections of the test site area towards the Glarey spring, where the isoclinal syncline connecting the Diablerets nappe and the Mt. Gond nappe is clearly visible. Note that the Cretaceous stratigraphy is more detailed than in the geological map (Fig. 2), which also shows the cross-section trace

Stratigraphy, paleokarst development, and rockfall

The Diablerets nappe below the Tsanfleuron karrenfield (lapiaz) is ~1,200 m thick; 150 m are due to tectonic repetition by an internal low-angle thrust that obliquely cuts most of the series (Fig. 3). The stratigraphy is well exposed in the high cliff SW of the lapiaz and comprises Middle and Upper Jurassic, Lower Cretaceous and Tertiary sedimentary formations.

The sequence starts with 60–100 m of Middle Jurassic (Dogger) black pelites (Aalenian), clayey siltstones, fine-grained sandstones and calcarenites. The overlying Upper Jurassic and Cretaceous series is principally composed of four limestone formations (two of which are in direct contact) separated by two thick marly formations, described, from base to top, as follows:

- Massive, micritic limestone of 200 m thickness (Malm)
- With a sharp stratigraphic contact follows a 200–250 m thick alternation of marls and mudstones of earliest Cretaceous age (Berriasian)
- This alternation gradually passes into a 150 m thick formation of bioclastic calcarenites (Late Berriasian to Valanginian)
- Above a sharp contact follows 150 m thick siliceous limestone (Hauterivian)
- With clear contact follows a 100 m thick alternation of marls and marly limestones (Early Barremian)
- This alternation passes upwards into the 120-m-thick Urgonian formation (Late Barremian to Early Aptian), consisting of massive and pure limestone that is quite resistant to mechanical erosion, but highly karstifiable, as discussed in the introduction

A major stratigraphic gap, resulting from uplift and regression starting at the beginning of the Palaeogene, separates the Urgonian from the overlying Eocene to Oligocene formations. The ensuing erosion removed the entire Upper Cretaceous, leaving the Urgonian limestone exposed at the surface. The overlying sediments represent a marine transgression and include, from base to top: sporadic continental (karstic and lacustrine) deposits; brackish sediments (Weidmann et al. 1991); shallow marine sandstones and nummulitic limestones (Menkveld-Gfeller 1994); Globigerina marls; and finally flysch, consisting of sandstone with abundant volcanic rock debris. The nummulitic limestone looks similar to

 DOI 10.1007/s10040-009-0485-4

the Urgonian limestone and is also karstifiable, but can be distinguished by means of fossils. In the study area, the total thickness of the Palaeogene sediments never exceeds 100 m.

Sporadic but sometimes spectacular paleokarst can be observed both on top and inside the Urgonian limestone. It formed during the continental period preceding the Eocene transgression mentioned above. Paleodolines, karren and solutionally-enlarged fractures are filled by continental (often residual) sediments such as fine-grained, iron-rich sandstones (Wieland 1976). Similar paleokarst phenomena have been studied more thoroughly in the Morcles nappe (Masson et al. 1980; Linder 2005).

At its SW margin, the Tsanfleuron karrenfield breaks off in steep cliffs from 2,900 m to 1,400 m asl, exposing the entire stratigraphic sequence (Fig. 2). A rockfall of 5×10^6 m^3 precipitated from these cliffs in 1714, destroying the village of Derborance. The Swiss writer C. F. Ramuz wrote a novel about this disaster (*Derborance*), but there is little scientific literature available.

Fault tectonics

Fractures of different types and age are numerous in the study area (Franck et al. 1984). The oldest are synsedimentary, revealed by abrupt variations of layer thickness and, occasionally, by the presence of pebbles and blocks. These fractures were active before and during the deposition of the Eocene sediments and have influenced paleokarst development, as demonstrated by paleodolines in the Urgonian limestone aligned along an ENE direction. Paleokarst development was stopped by the marine transgression, and then by the thrusting of the overlying nappes. Kinematic reconstructions suggest a tectonic overburden of 12 to 14 km (Escher et al. 1993).

The Rhône-Simplon Line is a major tectonic discontinuity, which follows the Rhône valley and splits into a number of ENE–WSW to E–W dextral strike-slip faults (Steck and Hunziker 1994; Steck et al. 1999). Some of these faults nearly reach the study area such as a prominent 15 km long fault known as the "CCA fault", which has a displacement of 200 m east of Tsanfleuron and branches westward into a multitude of minor fractures (Badoux et al. 1959).

In the Tsanfleuron area, just as in the entire region, the main system of relatively young (i.e. post-nappe) extensional fractures and small-scale conjugate shear zones indicates a stress field with a NW–SE (130–160°) maximum compression. This stress field is still active today, as revealed by focal mechanisms of numerous micro-earthquakes recorded along a seismic zone approximately following the CCA fault (Pavoni 1980; Franck et al. 1984; Pavoni et al. 1997). The influence of this fault zone on groundwater circulation can be observed in a nearby gallery (Rawil), which encountered a zone of water-bearing fissures between two dry sectors when crossing the CCA fault (Badoux 1982).

Geomorphologic zones of karst development

The Urgonian limestone outcrops of the Tsanfleuron area can be subdivided into three zones of karst development, also characterised by different recharge processes (see Fig. 4 and the following). Zone I is where the retreating glacier overlies the limestone. Zone II is located between the glacier front and the end moraine of 1855/1860, which indicates the glacier front during the 'Little Ice Age' (Greene et al. 1999; Hubbard et al. 2000). This zone offers the opportunity to observe limestone recently exposed by the glacier and to infer the structure of the ice–rock interface below the glacier. Polished rock surfaces predominate, partly covered by some rock debris representing a thin and patchy melt-out till. There are also meander karren, solutionally enlarged faults, vertical shafts, and large rocky depressions, often hundreds of meters wide and tens of meters deep. Conspicuous elongated calcite crystals on the limestone surface near the glacier front have formed below the ice, as described by Hubbard and Hubbard (1998).

Zone III, below the end moraine, constitutes a typical alpine karrenfield that formed since the end of the Pleistocene glaciations, uninterrupted by the Little Ice Age, similar to many other alpine karst systems. A great variety of karren and other karst landforms can be observed, with a soil and vegetation cover that increases with decreasing altitude. The differences between zones II and III are not only due to the Little Ice Age but also reflect a general change in karst development with altitude and temperature. Small lakes in zone II and small wetlands in zone III are due to paleodolines filled with low permeability deposits, as described above.

There are about 100 caves in the area, most of which are very small but some approach 1 km in length. With one exception, none of these caves reaches the active conduit network of the karst aquifer. Although caving teams have done much work, the regional speleological inventory is far from being completed. Most caves developed in Urgonian limestone, but some are also present in Eocene limestone. Cave entrances often consist of vertical shafts, but many caves also include subhorizontal passages, parallel to the stratification.

Hydrogeology

Hydrostratigraphy: aquifers and aquicludes

The sequence of aquifers and aquicludes can be inferred from the stratigraphy described above and illustrated in Fig. 3, complemented by field observations. The most important aquifer is the pure, competent, intensively fractured and karstified Urgonian limestone, which outcrops on large parts of the land surface. The limestone within the locally overlying Eocene and Oligocene formations is also karstified. Hydrological and speleological observations indicate that the two limestones form a connected karst aquifer.

The underlying Barremian marls constitute a regional aquiclude in other parts of the Helvetic zone (e.g.

 DOI 10.1007/s10040-009-0485-4

Goldscheider 2005). However, the thickness of this formation is only 100 m in the Tsanfleuron area and has partly been reduced due to tectonic movements as can be seen in the profile in Fig. 3; furthermore, the vertical displacements of some faults exceeds the thickness of this formation. Therefore, the hydraulic effectiveness of this formation as an aquiclude is not immediately apparent.

Below the Barremian marls follow Hauterivian siliceous limestone, Late Berriasian to Valanginian limestone (bioclastic calcarenites), Berriasian marl, and Malm limestone. In other regions of the Alps and Jura Mountains, the Malm forms a major regional karst aquifer (e.g. Herold et al. 2000); however, it is not immediately obvious if the Malm limestone and the Berriasian to Hauterivian limestones are actually karstified in the Tsanfleuron region. Karstification requires water circulation, but the entire sequence below the Barremian marls appears to be largely shielded against recharge and outcrops only in the steep cliffs south of the Tsanfleuron karrenfields (Fig. 2). However, springs that emerge from these limestone formations indicate karstification (see the following). Deep sub-vertical faults might form hydraulic connections from the land surface down towards the deeper limestone aquifers, across the entire stratigraphic sequence—a hypothesis that was later confirmed by tracer tests.

Recharge processes

A great variety of recharge processes can be observed in the Tsanfleuron-Sanetsch area (Fig. 4), some of which are specific to glacierised karst aquifer systems and have rarely or never been described in the literature. The recharge processes are related to the geomorphologic zones of the Urgonian limestone described above, and are closely linked to the meltwater production and drainage system of the Tsanfleuron glacier.

Glaciers typically consist of an accumulation zone and an ablation zone. During the past few years, the entire surface of the Tsanfleuron glacier often acted as an ablation zone, i.e. the firn line was above the highest point of the glacier, which means that the glacier is not simply retreating but vanishing. The northern sector of the glacier has a pronounced glacier tongue, and a glacier mouth that gives rise to the principal glacier stream, the Lachon. The southern sector consists of a shallow ice sheet on top of the karst limestone (Hubbard et al. 2000).

Numerous meltwater streams can be observed at the glacier surface during summer (supra-glacial drainage). Some of them sink into so-called moulins (glacial swallow holes). The moulins in the northern sector are probably connected to the glacier mouth and are thus tributary to the Lachon stream, while those in the southern sector are most likely connected to swallow holes below the glacier, i.e., the meltwater contributes to subglacial point recharge of the karst aquifer. Many paleo-subglacial swallow holes can be observed below the recent glacier front.

The Lachon glacier stream displays significant seasonal and diurnal discharge variations. Below the glacier mouth, it first flows over moraine and then over Urgonian limestone, where it sinks underground via swallow holes at different places, depending on the hydrologic conditions (Fig. 4). Only during the maximum early-summer snowmelt or storm rainfall does it form a continuous stream, ultimately a tributary of the Rhone River.

In the southern sector, many supra-glacial meltwater streams reach the glacier front, where they join with emerging subglacial meltwaters that flow at the ice–rock interface, sometimes as sheet flow. Below the glacier front, these meltwater streams first flow over limestone for short distances (typically tens of meters), often via meander karren or over polished rock surfaces, and then sink into swallow holes, often in the form of vertical shafts (Fig. 5). Due to the rapid glacier retreat, this is the most rapidly changing zone in the entire area.

Similar recharge processes can be observed in the entire zone II during snowmelt or intense rainfall, when innumerable streams flow over limestone for short distances before sinking underground via swallow holes. This is a fundamental difference between zone II and zone III, where all water immediately infiltrates though the epikarst zone. The diffuse infiltration and percolation of water through soil and epikarst has already been studied (e.g. Pronk et al. 2009), while recharge into glacier-polished limestone has rarely been described in detail.

The karst aquifer also receives allogenic recharge from the adjacent non-karst area to the east, mostly via streams that sink underground when they reach the karst area (Fig. 4). As this zone is used for cattle pasture, the swallow holes represent a potential source of microbial spring water contamination, as was demonstrated for other karst systems (Pronk et al. 2006).

Main springs

Five main springs drain the Tsanfleuron-Sanetsch karst aquifer system (Fig. 4). Small springs that are not relevant for regional drainage are not described here.

The Glarey spring—Swiss Coordinates: 589’650; 128’650; altitude: 1,553 m asl—is situated on the axis of the syncline connecting the Diablerets and Mont-Gond nappes (Fig. 3). It is used as a drinking water source for the community of Conthey, and for irrigation. Water from the Urgonian-Eocene karst aquifer is captured by means of a 30-m-long artificial drainage gallery with multiple branches. In winter, the mean discharge and specific electrical conductivity (SEC) are 30 L/s and 450 μS/cm, respectively, while higher mean discharge (180 L/s) and lower SEC (100 μS/cm) occur during summer, due to snow and glacier melt; the water temperature is relatively stable at 4°C. When the discharge of the main spring exceeds 40 L/s, an overflow spring becomes active, directly discharging into the Lachon stream 100 m upstream of the main spring. Both springs show identical diurnal variations of physicochemical characteristics. The discharge of the overflow can exceed 3,000 L/s, but has only been measured continuously by means of a pressure probe since 2008. For earlier years, it is possible to

 DOI 10.1007/s10040-009-0485-4

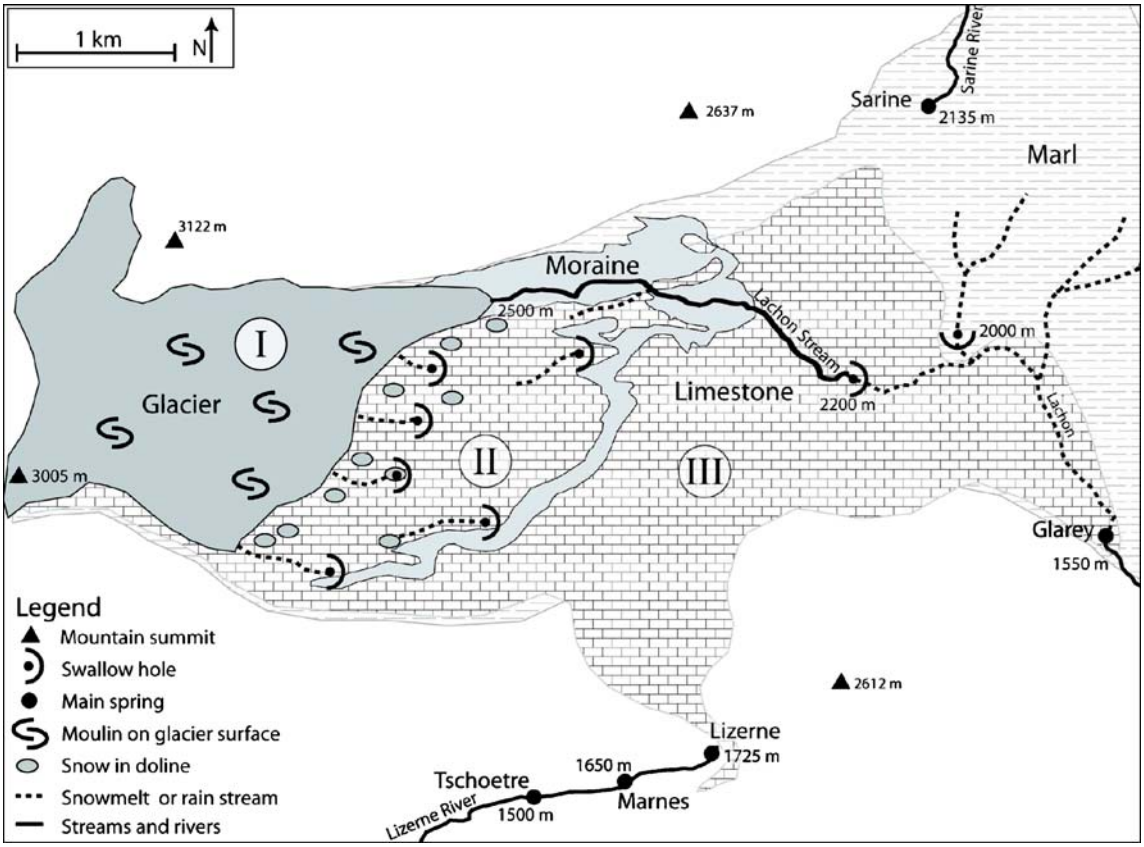

Fig. 4 Generalised hydrological map of the Tsanfleuron-Sanetsch area, showing the glacier and its moulins, the different recharge processes, the surface streams, swallow holes and springs. *Roman numbers* indicate the geomorphologic and recharge zones: *I* limestone covered by glacier, *II* polished limestone recently exposed by retreating glacier, *III* typical alpine karrenfield, below the end moraine of 1855/1860

reconstruct estimates of the overflow discharge using an empirical relation between the discharge of the main spring and the overflow that has been established in 2008.

Tschoetre spring—585′375; 127′075; 1,500 m—and Marnes spring—586′070; 127′150; 1,650 m—are located near the limit between the Malm karst aquifer and the Dogger aquiclude, which outcrops twice due to tectonic repetition (Fig. 2). Lizerne spring—586′355; 127′195; 1,725 m—discharges from the base of the Valanginian limestone. The mean annual SEC and temperature of the

Fig. 5 Swallow hole directly below the glacier front in the southern sector of the Tsanfleuron glacier, where it forms a shallow ice sheet. Due to rapid glacier retreat, new swallow holes are exposed every year, while previously active swallow holes get disconnected from the glacier (photo: N. Goldscheider)

 DOI 10.1007/s10040-009-0485-4

Tschoetre spring are 200 μS/cm and 5°C, respectively. As the spring forms a waterfall in a steep gorge, discharge measurements are difficult. The estimated mean discharge during summer is 500 L/s. The two other springs directly discharge into the Lizerne stream; measurements of electrical conductivity, temperature and discharge are not available.

The Sarine spring—588′400; 131′900; 2,135 m—is located north of the Sanetsch pass and seems to discharge from Berriasian marl near the base of the Mt. Gond nappe, not far from the thrust contact to the tectonically underlying Urgonian limestone of the Diablerets nappe. The mean spring discharge is 150 L/s; much higher than could be expected from a marl formation, suggesting inflow from a karst aquifer. However, the discharge is stable, and SEC (200 μS/cm) and water temperature (3°C) show no significant variability. All springs show similar chemical composition, with Ca^{2+}, Mg^{2+} and HCO^{3-} as the main ions, which is typical for groundwater from limestone and marl stratigraphy.

Tracer tests

Overview and experimental design

Between 2005 and 2008, 19 tracer injections were carried out in the Tsanfleuron area, in order to delineate the catchments of the five main springs, to determine transit times and flow velocities, to obtain information about interactions between the glacier, surface waters and groundwater, and to assess the possible impacts of contaminant releases on the Glarey spring.

Four different fluorescent dyes were used as tracers, due to their favourable properties (Käss 1998): Uranine, Sulforhodamine B and G, and Tinopal. Uranine was the preferred choice for single tracer tests, but Sulforhodamine B or G was used when two injections were too close in time. Uranine and Sulforhodamine B were used for multi-tracer tests with two injection points; Tinopal was used as the third tracer. Table 1 summarises the injection points (Nos. 1–19), the tracer types and quantities, and the experimental conditions. Figure 6 shows the location of the injection points, along with the results that will be discussed in the next section.

Injection No. 1 is the release of Tinopal into a cave stream that seems to show relatively little flow variations. The injection was done by a speleologist. Tracer test No. 2 is the injection of Uranine into the washbasin of the Prarochet mountain hut. Systematic flushing with tap water lasted only about 30 min; afterwards, flushing occurred in an irregular manner, as a function of the use of the washbasin. This tracer test also aimed at assessing the potential impact of the mountain hut on the Glarey spring.

Injection points No. 3–5, 12, 13, 17 and 18 are located near the southern and eastern margin of the glacier, where numerous small meltwater streams sink into karstified limestone. At several other sites, naturally flowing water is usually not available. Injection points No. 6–8 are dry dolines, shafts or inactive swallow holes. For the tracer injections, several m^3 of flushing water were delivered by tank trucks. Sites No. 9 and 10 are inaccessible for vehicles so that the injections were done during rainfall and snowmelt.

On four occasions, a tracer was injected into the main glacial stream (Lachon) at the glacier mouth (injections No. 11 and 14–16) in order to determine transit times between the glacier and the Glarey spring during different flow conditions. The main swallow holes are 3 km downstream (Fig. 4) so the tracers were exposed to sunlight and, thus, photolytic decay. Therefore, calculated tracer recoveries represent minimum values, as indicated in Table 1. A degradation experiment at this altitude revealed an Uranine loss of 40% in 5 h under sunlight. As a function of the different hydrological and meteorological conditions, degradation was lower for injection No. 11 but very high for injection No. 16. Sulforhodamine G, used for injection No. 15, is known to be less sensitive to daylight (Käss 1998). Experiment No. 19 is the injection of Uranine directly into the main swallow holes of the glacial stream, in order to avoid photolytic decay and to obtain realistic values of tracer recovery.

Springs were sampled for up to three weeks after injection, which is sufficient in this karst area where transit times are very short. Automatic samplers (ISCO), manual sampling, field fluorimeters (GGUN-FL30) and charcoal bags were used for monitoring. All water and charcoal samples were analysed in the CHYN laboratory (Neuchâtel, Switzerland) with a spectrofluorimeter (Perkin Elmer LS 50 B). The field fluorimeters measure the dye concentration in the spring water at user-selectable time intervals ranging from 2 s to 15 min.

Presentation and discussion of the tracer results

Positive results were obtained for all of the 19 tracer tests. Table 1 presents a summary with the times of maximum concentration (peak times), the maximum normalised concentrations, the tracer recoveries and the linear distances between injection and sampling points. Figure 6 shows the connections demonstrated by tracer tests, and the peak times.

Only a few tracers arrived at more than one spring at the same time such as the Uranine injected into No. 7, which was detected both at the Glarey spring and the Sarine spring. Most other injection points are connected to one spring only; furthermore, the tracer flow paths do not cross each other, i.e., most proven connections are simple point-to-point connections. This helps to delineate the spring catchment areas, as shown in Fig. 6.

The tracer tests demonstrate that the catchment of the Glarey spring comprises large parts of the Tsanfleuron karrenfield and glacier, while the four other springs (Sarine, Marnes, Lizerne, and Tschoetre) drain only very marginal parts of the karrenfield with very small contribution of the meltwater from the glacier.

The transit times in the conduit system, obtained from the peaks of the breakthrough curves, are very short,

 DOI 10.1007/s10040-009-0485-4

Table 1 Summary of the experimental setup and results of the tracer tests in the Tsanfleuron area

Injection	1	2	3	4	5	6	7	8	9	10	11[a]	12	13	14[a]	15[a]	16[a]	17	18	19
Date	03 Sep 2005			18 Sep 2005		02 Aug 2006			13 Aug 2006	15 Aug 2006	24 Jul 2007			29 Aug 2007	30Aug 2007	11 Sep 2007	26 Jul 2008	07 Aug 2008	26 Aug 2008
Altitude(m)	2,300	2,555	2,847	2,700	2,845	2,128	2,249	2,284	2,197	2,460	2,439	2,532	2,603	2,439	2,382	2,439	2,840	2,196	2,196
Tracer	Tin	Ur	SB	SB	Ur	Tin	Ur	SB	Ur	SB	Ur	SB	Tin	Ur	SG	Ur	Ur	SB	Ur
Mass(g)	2,000	200	450	500	500	2,000	300	500	1,000	1,000	200	500	2,000	300	700	600	1,000	1,000	200
Precipitation	-	-	-	-	-	+	+	+	+	+	+	+	+	++	+	-	-	-	-

Sampling site (altitude)	Results from tracer injection n°																			Quantity (unit)
	1	2	3	4	5	6	7	8	9	10	11[a]	12	13	14[a]	15[a]	16[a]	17	18	19	
Glarey spring (1,553 m)	2,500 31.4 88.8 ~ 80	4,400 54.8 8.93 ~ 50	ND	5,900 57 70.5 ~ 95	ND	2,000 33.0 2.9 ~ 65	3,150 29.5 3.3 ~ 20	ND	ND	ND	5,213 5.8 31.4 ~ 50	4,945 10.3 1.8 ~ 5	5,196 12.8 ?[b] ?[b]	ND[c]	4,848 5.4 29.9 ~ 55	5,213 15.3 7.4 ~ 20	6,250 12.9 46.1 ~ 40	ND	2,274 6.1 69.8 ~ 75	d (m) t (h) c/M ($10^{-6}m^{-3}$) R (%)
Sarine spring (2,135 m)	ND	ND	ND	ND	ND	ND	590 37.0 2.9 0.8	1,227 11.5 240 71.4	*NS*	*NS*	ND	ND	ND	X	ND	ND	*NS*	*NS*	*NS*	d (m) t (h) c/M ($10^{-6}m^{-3}$) R (%)
Tschoetre spring (1,500 m)	ND	ND	2,900 16.2 17 ~ 47	ND	3,100 32.3 21.2 ~ 35	*NS*	*NS*	*NS*	*NS*	*NS*	ND	ND	ND	*NS*	*NS*	*NS*	ND	ND	*NS*	d (m) t (h) c/M ($10^{-6}m^{-3}$) R (%)
Marnes spring (1,650 m)	*NS*	*NS*	*NS*	*NS*	*NS*	*NS*	*NS*	*NS*	X	X	*NS*	*NS*	*NS*	*NS*	*NS*	*NS*	ND	X	*NS*	
Lizerne spring (1,725 m)	*NS*	*NS*	*NS*	*NS*	*NS*	*NS*	*NS*	*NS*	X	X	*NS*	*NS*	*NS*	*NS*	*NS*	*NS*	ND	NS	*NS*	

Tracers: *Tin* Tinopal, *Ur* Uranine, *SB/SG* Sulforhodamine B/G. Precipitation: –, + and ++ mean no, moderate and intense rainfall, respectively. Results include tracer recovery (*R*), time of maximum concentration (*t*), normalised maximum concentration (*c/M*) and distance (*d*). *ND* sampled but not detected. *X* connection demonstrated by means of charcoal bags. *NS* not sampled

[a] Exposure to sunlight and photolytic decay. Recoveries are minimum values

[b] Due to interferences with organic carbon, Tinopal concentrations and recovery cannot be determined

[c] Due to very high flow rates, the main swallow hole of the Lachon stream probably acted as a spring, so that the tracer did not enter the aquifer

DOI 10.1007/s10040-009-0485-4

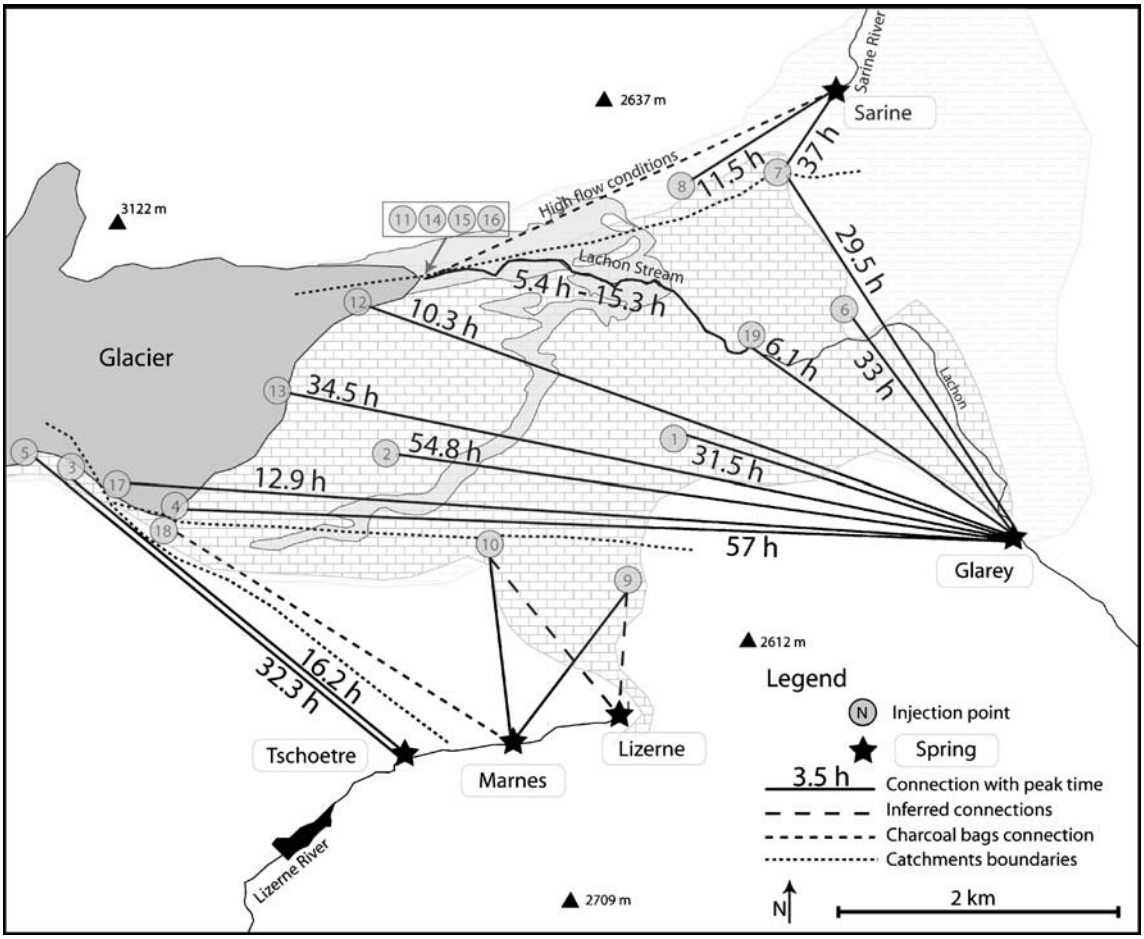

Fig. 6 Underground connections demonstrated by tracer tests with peak times and catchments boundaries. See also Fig. 4 legend

ranging from 5.4 to 57 h. The shortest times were observed between the main glacier stream (Lachon) and the Glarey spring (injections No. 11, 15 and 19), suggesting that the principal swallow hole of this stream is connected to a well-developed karst conduit. In the catchment of the Glarey spring, there is no correlation between distance and transit time, which illustrates the high degree of heterogeneity that is characteristic for karst aquifer systems. For example, the tracer injected at site No. 1 took 31.4 h for a 2,500 m linear distance, while tracer No. 17 took 12.9 h for 6,250 m (Table 1; Fig. 6).

Tracer recoveries at the Glarey spring (including the contribution of the overflow), range from ~5% (No. 12) to ~96% (No. 4). High recoveries indicate a straightforward conduit connection between the injection point and the spring. Lower recoveries may have different reasons, such as photolytic decay for injections No. 11, 15 and 16, or tracer loss at the injection site due to the absence of naturally flowing water (Nos. 6 and 7). However, when a conservative tracer is directly injected into the conduit network, typically via a swallow hole, recoveries can be used to obtain additional information on the underground flow system. Recoveries lower than 100% mean that the missing part of the tracer and water went elsewhere. In the present case, the low recoveries for some of the injected tracers may indicate deep infiltration into subvertical fractures and/or continued flow in the Urgonian karst aquifer towards the east, where the Diablerets nappe plunges under the tectonically higher nappes.

The rapid connections from injection points Nos. 3 and 5, located at the top of the Urgonian limestone karrenfield at ~2,850 m altitude, towards the Tschoetre spring, which discharges from the Malm aquifer at 1,500 m, shows that deep infiltration via fractures does actually occur across the entire stratigraphic sequence.

Some breakthrough curves (BTCs) show multiple peaks with 24-h periodicity, indicating an influence of glacier melt. Figure 7 presents two BTCs observed at the Glarey spring during the same multi-tracer test, i.e. during identical hydrological conditions. Uranine was injected into the washbasin of the mountain hut (No. 2), and Tinopal into a cave stream (No. 1). Both tracers arrived at the spring after about 30 h (time of first detection); the Tinopal BTC essentially shows a single peak, while Uranine displays at least six peaks in 24-h intervals. It is hypothesised that the Uranine was transported through the unsaturated zone towards an active karst conduit directly connected to the glacier. The diurnal variability of water level and flow rate in this conduit causes a stepwise mobilisation of the tracer; intense rainfall on the eighth day seemed to wash out the

 DOI 10.1007/s10040-009-0485-4

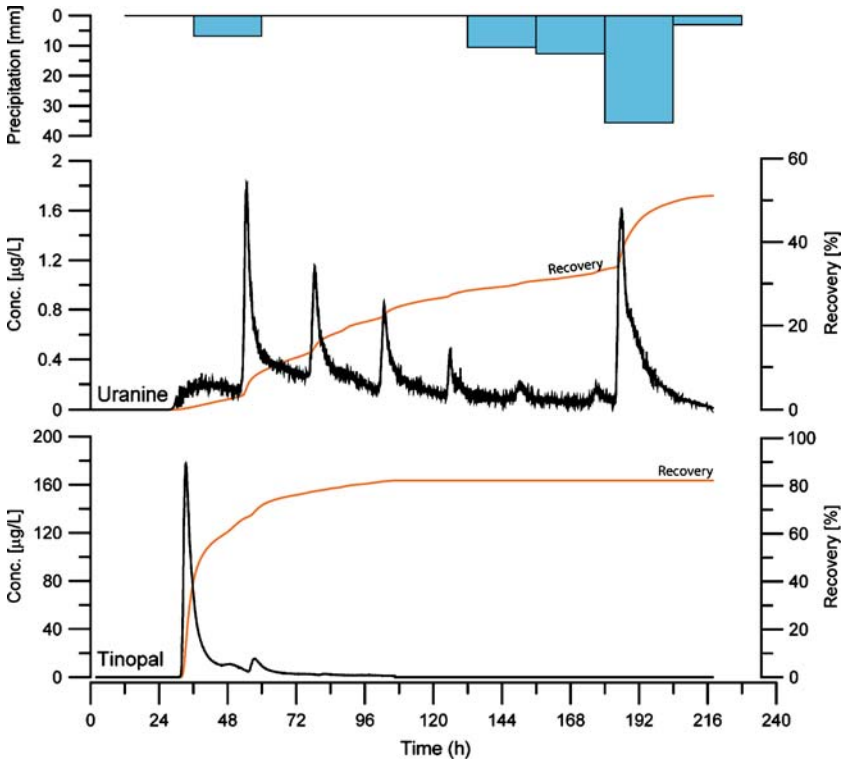

Fig. 7 Breakthrough curves monitored at the Glarey spring, along with recoveries and daily precipitation, resulting from the injection of Tinopal (injection No. 1 in Table 1 and Fig. 6) and Uranine (No. 2) on the same day. Both tracers were first detected after about 30 h. Uranine shows several peaks in 24-h intervals, indicating influence of the diurnal variations of glacier melt; further explanations in the text

remaining tracer, illustrated by an additional and final Uranine peak. Tinopal, on the other hand, was transported in a cave stream far away from the glacier without intermediate storage in the unsaturated zone and without significant diurnal variability.

The connections from injection points No. 9, 10 and 18 to the Marnes spring were established by very high tracer concentrations found in charcoal bags placed downstream in the Lizerne River. Tracers No. 9 and 10 were also detected in a charcoal bag that was placed upstream from the spring, but at lower concentration levels. This finding pointed to the presence of an important spring farther upstream, the Lizerne spring, which was previously unknown.

Although discharge is not monitored at the inaccessible Tschoetre spring, the multi-peak Uranine BTC resulting from injection No. 5 clearly illustrates the influence of the diurnal variability of glacier melt on this spring (Fig. 8). The tracer pathway crosses several unsaturated limestone and marl formations, obviously along deep vertical fractures, before it reaches the active flow system of the Marl karst aquifer. Intermediate tracer storage in the unsaturated zone and periodic flushing by meltwater can explain the observed BTC.

The tracer injections in the Lachon stream near the glacier mouth made it possible to better characterise the glacier–stream–aquifer–spring relations during different hydrologic conditions (Fig. 9). As just described, the tracers were exposed to daylight between the injection site and the swallow hole so that partial photolytic decay had occurred. During low-flow conditions (injection No. 16), the tracer peaked after 15 h but the recovery was only ~20%, indicating substantial photolytic decay in the slow-flowing surface stream. During high-flow conditions (No. 11), the maximum tracer concentration occurred only 5 h after injection and the recovery was substantially higher (50%) indicating less tracer loss by photolytic decay due to shorter residence times in the stream. Due to the short transit times (the breakthrough was largely completed within about 15 h), the BTC from this injection shows no discernible influence of the diurnal glacier-melt variations, unlike the BTCs presented in Figs. 7 and 8. During very

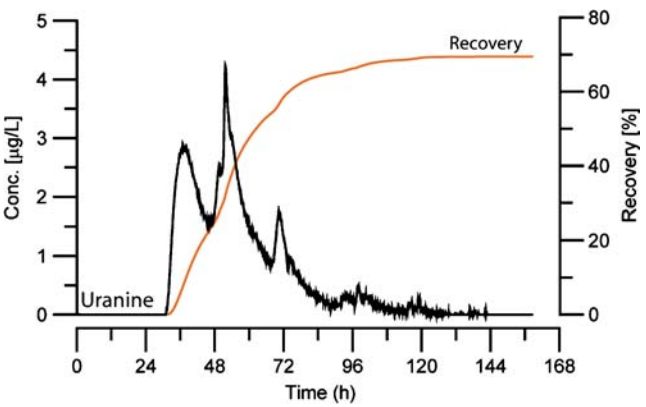

Fig. 8 Uranine breakthrough curve monitored at Tschoetre spring, resulting from injection No. 5. The multi-peak behaviour is attributed to the diurnal variability of glacial meltwater production

 DOI 10.1007/s10040-009-0485-4

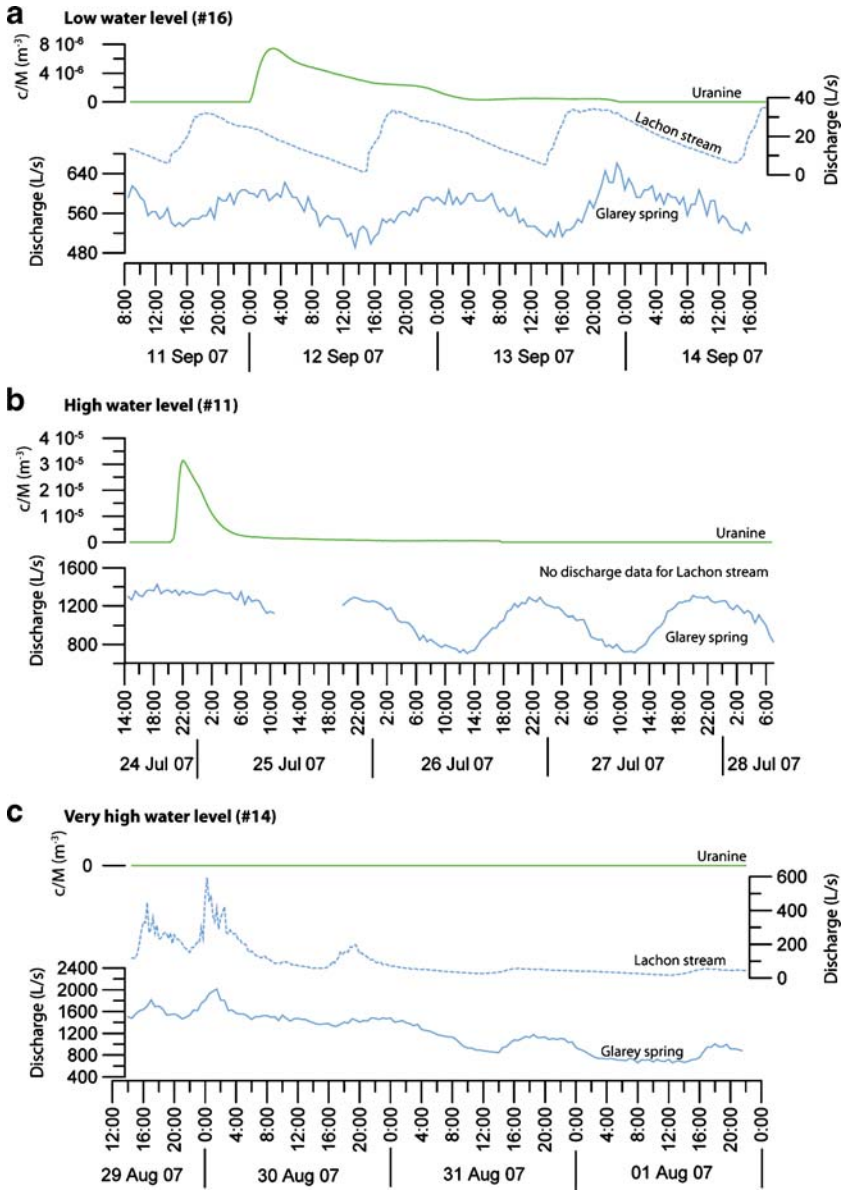

Fig. 9 Discharge monitored at the Glarey spring and the Lachon stream (if available) during three different tracer tests carried out during different hydrologic conditions, and resulting Uranine BTCs, monitored at the Glarey spring: **a** injection No. 16, **b** injection No. 11 and **c** injection No. 14 (see also Table 1 and Fig. 6). During high-flow conditions, shorter transit times and a higher recovery were observed than during low-flow. During very high flow conditions, the tracer did not reach the spring as the swallow holes were obviously not active. *c/M* is the uranine concentration normalized by the injected mass

high flow conditions, when little photolytic decay is expected, the tracer did not arrive at the spring, indicating that the swallow holes were not active but probably transformed into springs, i.e. they act as estavelles.

Conceptual model of karst drainage

Based on geological considerations, hydrologic observations and tracer test results, a conceptual model of the underground drainage pattern of this glacierised karst aquifer system was established as illustrated in two hydrogeological sections (Figs. 10 and 11).

The Urgonian and Eocene limestones constitute the main regional karst aquifer. The underlying Barremian marl forms an aquiclude, which is, however, relatively thin (~100 m). Various processes contribute to aquifer recharge, including sinking streams from adjacent non-karst areas (allogenic recharge), diffuse infiltration of rain and snowmelt water, infiltration of glacial meltwater underneath the glacier and near its front, as well as sinking of the main glacier stream far downstream from the glacier mouth (autogenic recharge).

Large parts of the area are mainly drained by the Glarey spring, but marginal zones drain towards four other springs (Fig. 6). Structurally, the aquifer forms a large anticlinorium with a poorly defined axis and a wide crest,

 DOI 10.1007/s10040-009-0485-4

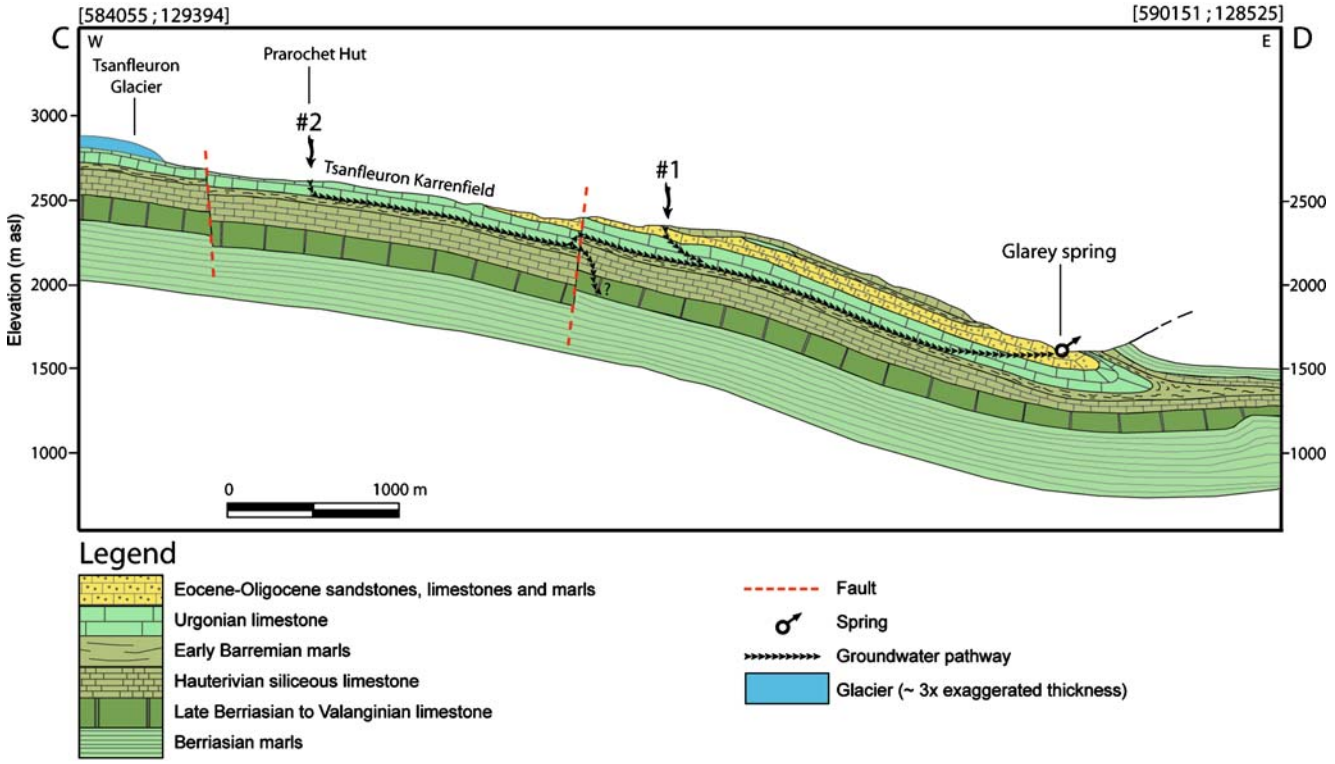

Fig. 10 Conceptual model of karst drainage from the Tsanfleuron glacier and karrenfield towards the Glarey spring, confirmed by tracer tests (injection points No. 1 and 2 are shown, also see Fig. 6). Water flow occurs near the base of the Urgonian-Eocene karst aquifer on top of the underlying Barremian marl towards the isoclinal syncline that collects all water and conveys it to the spring. Infiltration into deeper aquifers along faults is assumed (section line see Fig. 2)

plunging towards the ENE below tectonically higher nappes, with an axial plunge of 5–10°. The southward adjacent isoclinal syncline, on the other hand, has a well-defined axis and forms a narrow trough. The Glarey spring is located where a deeply incised valley cuts this syncline at a low topographic position (1,553 m).

It is assumed that underground drainage essentially occurs near the base of the shallow karst aquifer, on top of the underlying marl, and follows the fracture network and the dip of the strata (Fig. 10). The karst waters partly flow towards the ENE, following the gentle plunge of the anticlinorium, but eventually turn southward, where the isoclinal syncline acts as a major drainage structure, collecting and conveying the water towards the Glarey spring.

Some tracer tests resulted in high recoveries, indicating straightforward connection between the respective swallow holes and the Glarey spring, via well-developed conduits. Other tracers, although directly injected into the conduit network via swallow holes, reappeared at substantially lower recoveries (sometimes only 5%), suggesting that the remaining part of the tracer and, thus, an important part of the water, went elsewhere. It is generally known that high mountain areas often act as recharge zones for large, deep groundwater circulation systems (Toth 1963, 1999). However, infiltration into these systems can rarely be directly observed. In the Tsanfleuron-Sanetsch area, two types of deep infiltration can be hypothesised, supported by geological and hydrological considerations, and tracer test evidence:

1. Continued groundwater flow in the Urgonian-Eocene karst aquifer following the general plunge of the Diablerets nappe towards the ENE
2. Deep infiltration via subvertical fractures and faults, across the relatively thin Barremian marl aquiclude and the underlying formations

The first type can only be indirectly deduced from the geological structure and the low tracer recoveries, but cannot be observed directly, because the Diablerets plunges below tectonically higher nappes east of the Sanetsch pass and there are no accessible sampling points farther to the east where the re-emergence of groundwater from the study area could be observed.

The second type of deep infiltration, however, is confirmed by the two positive tracer tests between the surface of the Urgonian-Eocene karst aquifer and the Tschoetre spring, which discharges from the Malm karst aquifer, 1,350 m below (Fig. 11). Between the injection points and the spring, the tracers crossed about 800 m of marl and limestone stratigraphy in less than 2 days, which is only possible via open, subvertical fractures and faults. As a consequence of the steep topography in this part of the area, fractures probably opened by gravitation, enabling rapid water percolation. The catastrophic rockfalls, which plunged

 DOI 10.1007/s10040-009-0485-4

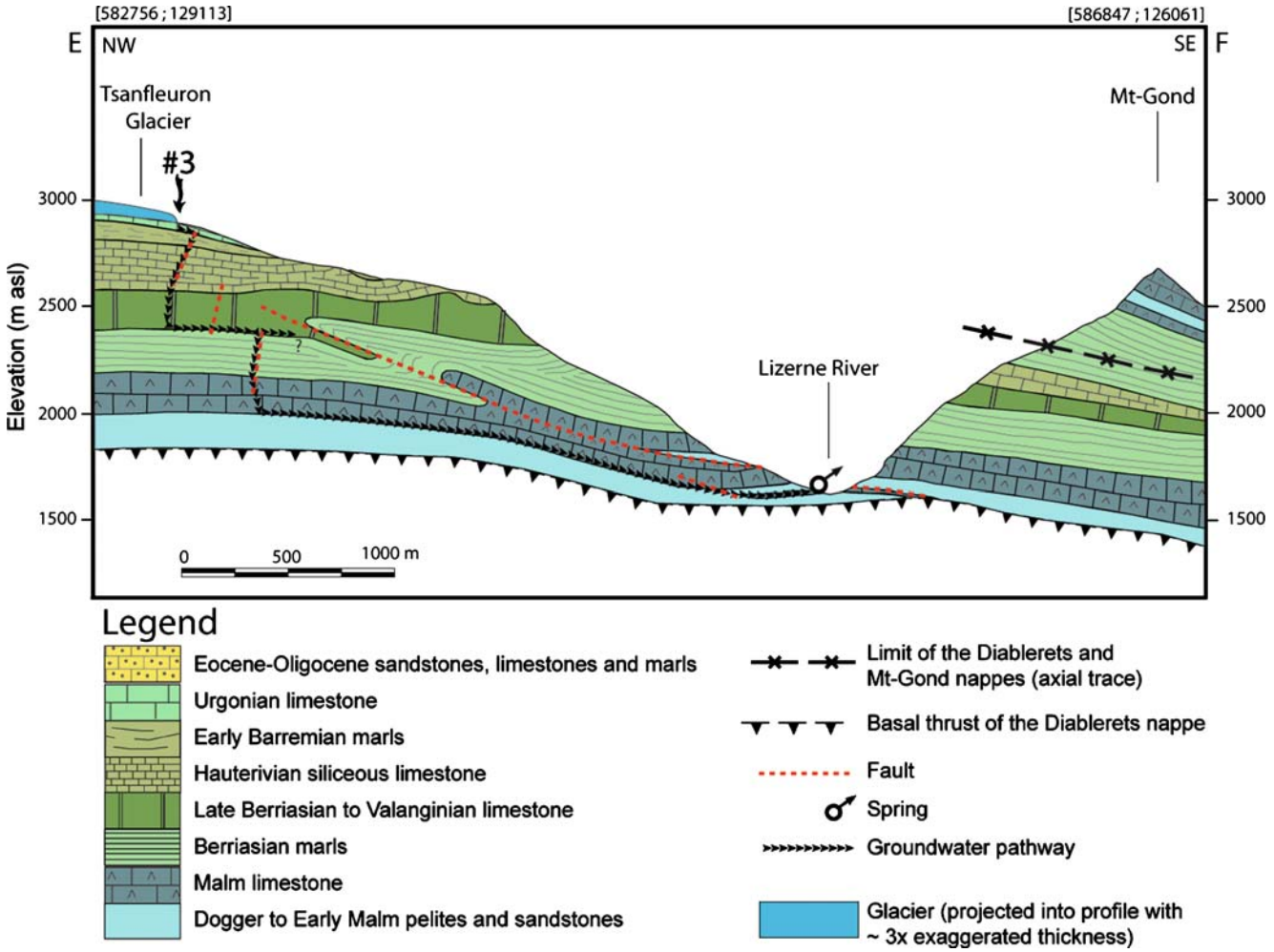

Fig. 11 Conceptual model of flow from the upper part of the Tsanfleuron glacier and karrenfield towards the Tschoetre spring, confirmed by tracer tests (injection point No. 3 is shown; see also Fig. 6). The tracer crossed the entire stratigraphic sequence, including several marl formations, in less than two days along deep fractures that opened due to the steep topography (glacier projected into section, see Fig. 2)

from these cliffs in 1714 and 1749, further support the supposed existence of open fractures.

Both the Tschoetre and the Glarey springs receive inflow from the glacier and rapidly react on the temperature-driven diurnal variations of meltwater production. Flow towards the Lizerne and Marnes springs follows pathways similar to those towards the Tschoetre spring, i.e. from the main karst aquifer along fractures across marl aquicludes towards Valanginian and Malm limestone aquifers, respectively.

The Sarine spring, located near the tectonic contact between two nappes, seems to discharge from Berriasian marl but receives inflow from the Tsanfleuron karst area, as demonstrated by tracer tests. The crest of the anticlinorium, although not precisely defined, acts as a water divide between the catchments of the Sarine spring and Glarey spring. One tracer injection went to both springs; during high flow conditions, there is also inflow from the glacier stream to the Sarine spring. The spring is characterised by high but stable discharge, and stable physicochemical parameters. It is hypothesised that the spring is connected to a karstified limestone imbricate thrust that drains the surrounding marl aquitards and is also connected to the main aquifer. More research is necessary to confirm this hypothesis.

Conclusions and outlook

Apart from the immediate relevance of a better understanding of regional hydrogeology and for the delineation of protection zones for the Glarey spring, the study also allows several conclusions of more general relevance to be drawn. Groundwater flow in alpine karst aquifer systems consisting of marl and limestone formations often follows the stratification. Therefore, fold structures have a major influence on groundwater flow in shallow karst systems, as already demonstrated by means of tracer tests in several alpine karst systems (e.g. Goldscheider 2005). Butscher and Huggenberger (2007) used geologic three-dimensional modelling in combination with a conceptual flow model approximating underground drainage of shallow karst systems by open surface flow on top of the underlying aquiclude. In the Tsanfleuron-Sanetsch karst system, the

 DOI 10.1007/s10040-009-0485-4

anticlinorium is part of the continental water divide between the catchments of the Rhone and Rhine rivers; the isoclinal syncline acts as a regional drainage structure, conveying water towards the Glarey spring.

Due to the presence of fractures and faults, there is also flow across the stratification. It was possible to demonstrate rapid flow across an 800 m sequence of marls and limestone, towards the Tschoetre spring, in less than 2 days. Catastrophic rockfalls occurred in this part of the area in historic times. The tracer tests indicate the presence of open fractures and thus the risk of future rockfalls, enhanced by permafrost thawing and glacier retreat.

Not all recharge water reappears at accessible springs, but a part of the water feeds deeper and larger regional flow systems. In the Tsanfleuron-Sanetsch area, two types of deep infiltration can be supposed, and partly demonstrated: (1) parallel to the stratification, following the plunge of the Diablerets nappe towards the ENE below tectonically higher nappes, and (2) across the stratification, along subvertical fractures, at least down to Malm limestone.

Intense interactions between the glacier and the karst aquifer, including specific recharge processes, were observed. The diurnal variations of the glacial meltwater production influence tracer transport in the aquifer, confirming the importance of hydrologic variability for contaminant transport processes in karst aquifer systems (Göppert and Goldscheider 2008). On the basis of this study, future research in this test site will focus on a better characterisation of the influence of the diurnal and seasonal variability of glacier melt upon groundwater flow (and sediment transport) in the aquifer using simple modelling approaches (e.g. Fleury et al. 2007). Finally, the project will develop prognoses for the impacts of climate-change induced glacier retreat on the availability and quality of freshwater from the spring.

Acknowledgements The Swiss National Science Foundation has funded the GLACIKARST project since 2004 (grant No. 200020-113609/1). The authors thank the community of Conthey for financial and logistic support, the caving teams for their help, several students and colleagues for their various contributions, particularly J. Nessi, S. Deyres, L. Tobler, K. Spiegelhalter, F. Bourret and R. Costa, and T. Bechtel for proofreading.

References

Badoux H (1982) Des événements de Zeuzier et de la galerie de sondage du Rawyl RN6 [The incidents of Zeusier and the exploration gallery of Rawyl]. Ingénieurs et Architectes Suisses. Bull Tech Suisse romande 12:155–167

Badoux H, Bonnard EG, Burri M, Vischer A (1959) Feuille St-Léonard et Notice explicative [Map sheet St-Léonard with explanatory note]. Atlas géol. Suisse 1:25000, no. 35, Service Géologique National, Bern

Badoux H, Gabus JH, Mercanton CH (1990) Feuille 1285 Les Diablerets [Map sheet 1285, Les Diablerets]. Atlas géol. Suisse 1:25000, no. 88, Service Géologique National, Bern

Boulton GS, Slot T, Blessing K, Glasbergen P, Leijnse T, Vangijssel K (1993) Deep circulation of groundwater in overpressured subglacial aquifers and its geological consequences. Quat Sci Rev 12(9):739–745

Butscher C, Huggenberger P (2007) Implications for karst hydrology from 3D geological modeling using the aquifer base gradient approach. J Hydrol 342(1–2):184–198

Crespo-Blanc A, Masson H, Sharp Z, Cosca M, Hunziker J (1995) A stable and $^{40}Ar/^{39}Ar$ isotope study of a major thrust in the Helvetic nappes (Swiss Alps): evidence for fluid flow and constraints on nappe kinematics. Geol Soc Am Bull 107 (10):1129–1144

Escher A, Masson H, Steck A (1993) Nappe geometry in the Western Swiss Alps. J Struct Geol (15):501-509

Fairchild I-J, Killawee J-A, Hubbard B, Dreybrodt W (1999) Interactions of calcareous suspended sediment with glacial meltwater: a field test of dissolution behaviour. Chem Geol 155(3–4):243–263

Fleury P, Plagnes V, Bakalowicz M (2007) Modelling of the functioning of karst aquifers with a reservoir model: application to Fontaine de Vaucluse (South of France). J Hydrol 345(1–2):38–49

Flowers GE, Bjornsson H, Palsson F (2003) New insights into the subglacial and periglacial hydrology of Vatnajokull, Iceland, from a distributed physical model. J Glaciol 49 (165):257–270

Franck P, Wagner JJ, Escher A, Pavoni N (1984) Evolution des contraintes tectoniques et sismicité dans la région du col du Sanetsch, Alpes valaisannes helvétiques [Evolution of tectonic constrains and seismicity in the Sanetsch region, Helvetic Valais Alps]. Eclogae Geol Helv 77(2):383–393

Goldscheider N (2005) Fold structure and underground drainage pattern in the alpine karst system Hochifen-Gottesacker. Eclogae Geol Helv 98(1):1–17

Göppert N, Goldscheider N (2008) Solute and colloid transport in karst conduits under low- and high-flow conditions. Ground Water 46(1):61–68

Greene AM, Broecker WS, Rind D (1999) Swiss glacier recession since the little ice age: reconciliation with climate records. Geophys Res Lett 26(13):1909–1912

Häuselmann P, Otz M, Jeannin P-Y (2003) A review of the dye tracing experiments done in the Siebenhengste karst region (Bern, Switzerland). Eclogae Geol Helv 96(1):23–36

Herold T, Jordan P, Zwahlen F (2000) The influence of tectonic structures on karst flow patterns in karstified limestones and aquitards in the Jura Mountains, Switzerland. Eclogae Geol Helv 93(3):349–362

Hubbard B (2002) Direct measurement of basal motion at a hard-bedded, temperate glacier: Glacier de Tsanfleuron, Switzerland. J Glaciol 48(160):1–8

Hubbard B, Hubbard A (1998) Bedrock surface roughness and the distribution of subglacially precipitated carbonate deposits: implications for formation at Glacier de Tsanfleuron, Switzerland. Earth Surf Proc Land 23(3):261–270

Hubbard B, Tison JL, Jannsens L, Spiro B (2000) Ice core evidence for the thickness and character of clear facies basal ice: Glacier de Tsanfleuron, Switzerland. J Glaciol 46(152):140–150

Hubbard B, Hubbard A, Tison J-L, Mader HM, Nienow P, Grust K (2003) Spatial variability in the water content and rheology of temperate glaciers: Glacier de Tsanfleuron, Switzerland. Ann Glaciol 37:1–6

Jeannin PY (2001) Modeling flow in phreatic and epiphreatic karst conduits in the Hölloch cave (Muotatal, Switzerland). Water Resour Res 37(2):191–200

Käss W (1998) Tracing technique in geohydrology. Balkema, Rotterdam, 585 pp

Kleinn J, Frei C, Gurtz J, Luthi D, Vidale PL, Schar C (2005) Hydrologic simulations in the Rhine basin driven by a regional climate model. J Geophys Res Atmos 110, D04102

Linder P (2005) An Eocene paleodoline in the Morcles Nappe of Anzeindaz (Canton de Vaud, Switzerland). Eclogae Geol Helv 98(1):51–61

Lugeon M (1914) Les Hautes Alpes calcaires entre la Lizerne et la Kander (Wildhorn, Wildstrubel, Balmhorn et Torrenthorn), I [The high limestone Alps between Lizerne and Kander]. Matér. Carte géol. Suisse (N.S.) 30, Francke, Bern, 360 pp

 DOI 10.1007/s10040-009-0485-4

Lugeon M (1940) Feuille Diablerets et Notice explicative [map sheet Diablerets with explanatory note]. Atlas géol. Suisse 1:25000, no. 19, Service Géologique National, Ber

Maréchal JC, Perrochet P, Tacher L (1999) Long-term simulations of thermal and hydraulic characteristics in a mountain massif: the Mont Blanc case study, French and Italian Alps. Hydrogeol J 7(4):341–354

Masson H, Baud A, Escher A, Gabus J, Marthaler M (1980) Compte rendu de l'excursion de la Société Géologique Suisse du 1 au 3 octobre 1979 : coupe Préalpes-Helvétique-pennique en Suisse occidentale [Minutes of the field trip of the Swiss Geologic Society on 1–3 October 1979: section of the Helvetic-Penninic Pre-Alps in western Switzerland]. Eclogae Geol Helv 73(1):331–349

Menkveld-Gfeller U (1994) Die Wildstrubel-, die Hohgant- und die Sanetsch-Formation: Drei neue lithostratigraphische Einheiten des Eocaens der helvetischen Decken [The Wildstrubel, Hohgant and Sanetsch Formations: three new lithostratigraphic units of the Eocene of the Helvetic nappes]. Eclogae Geol Helv 87(3):789–809

Paul F, Kaab A, Maisch M, Kellenberger T, Haeberli W (2004) Rapid disintegration of Alpine glaciers observed with satellite data. Geophys Res Lett 31 (L21)

Pavoni N (1980) Comparison of focal mechanisms of earthquakes and faulting in the Helvetic zone of the Central Valais, Swiss Alps. Eclogae Geol Helv 73(2):551–558

Pavoni N, Maurer H-R, Roth P, Deichmann N et al (1997) Seismicity and seismotectonics of the Swiss Alps. In: Pfiffner AO (ed) Deep structure of the Swiss Alps: results of NRP 20. Birkhäuser, Basel, pp 241–250

Pronk M, Goldscheider N, Zopfi J (2006) Dynamics and interaction of organic carbon, turbidity and bacteria in a karst aquifer system. Hydrogeol J 14(4):473–484

Pronk M, Goldscheider N, Zopfi J, Zwahlen F (2009) Percolation and particle transport in the unsaturated zone of a karst aquifer. Ground Water 47(3):361–369

Schaefli B, Hingray B, Musy A (2007) Climate change and hydropower production in the Swiss Alps: quantification of potential impacts and related modelling uncertainties. Hydrol Earth Syst Sci 11(3):1191–1205

Seidel K, Ehrler C, Martinec J (1998) Effects of climate change on water resources and runoff in an Alpine basin. Hydrol Process 12(10-11):1659–1669

Smart CC (1996) Statistical evaluation of glacier boreholes as indicators of basal drainage systems. Hydrol Process 10(4):599–613

Steck A, Hunziker J (1994) The Tertiary structural and thermal evolution of the Central Alps: compressional and extensional structures in an orogenic belt. Tectonophysics 238:229–254

Steck A, Bigioggero B, Dal Piaz GV, Escher A, Martinotti G, Masson H (1999) Carte tectonique des Alpes de Suisse occidentale et des régions avoisinantes 1:100000 [Tectonic map of the western Swiss Alps and neighbouring regions]. Special geological map no. 123, Service Géologique National, Bern

Steck A, Epard JL, Escher A, Gouffon Y, Masson H (2001) Carte tectonique des Alpes de Suisse occidentale et des régions avoisinantes 1:100000. Notice explicative [Tectonic map of the western Swiss Alps and neighbouring regions, explanatory note], Service Géologique National, Bern, 73 pp

Toth J (1963) A theoretical analysis of groundwater flow in small drainage basins. J Geophys Res 68(16):4795–4812

Toth J (1999) Groundwater as a geologic agent: an overview of the causes, processes, and manifestations. Hydrogeol J 7(1):1–14

Viviroli D, Weingartner R (2004) The hydrological significance of mountains: from regional to global scale. Hydrol Earth Sys Sci 8(6):1016–1029

Weidmann M, Franzen J, Berger J-P (1991) Sur l'âge des Couches à Cérithes ou Couches des Diablerets de l'Eocène alpin [About the age of the Cerithes or Diablerets formation of the alpine Eocene]. Eclogae Geol Helv 84(3):893–919

Wieland B (1976) Petrographie eozäner siderolithischer Gesteine des Helvetikums der Schweiz: ihre Diagenese und schwache Metamorphose [Petrography of Eocene siderolithic rocks of the Swiss Helvetic zone: their diagenesis and weak metamorphosis]. PhD Thesis, Univ. Bern, Switzerland, 117 pp

 DOI 10.1007/s10040-009-0485-4